Postprint of: Czaja Z., A New Approach to Capacitive Sensor Measurements Based on a Microcontroller and a Three-Gate Stable RC Oscillator, IEEE Transactions on Instrumentation and Measurement, Vol. 72 (2023), 2002009, DOI: 10.1109/TIM.2023.3244851

A New Approach to Capacitive Sensor Measurements Based on a Microcontroller and a Three-gate Stable RC Oscillator

Zbigniew Czaja, *Member, IEEE*

***Abstract*—A complete smart capacitive sensor solution based on a microcontroller was developed. This approach includes the development of both the hardware and software. The hardware part comprises an 8-bit microcontroller equipped with two timers/counters and a three-gate stable RC** relaxation **oscillator. The software part handles system configuration, measurement control, communication control, and data processing. Hence, the microcontroller acts as a frequency meter with an adaptive measuring time, and the relaxation oscillator generates a square wave with a frequency depending on the value of the capacitance of the sensor. The paper also proposes a calibration method that reduces the measurement range to 1 pF. The experimentally proven relative measurement errors of sensor capacitance are less than 0.012% for values smaller than 12 pF, and less than 0.0084% for values from 12 pF to 300 pF.**

***Index Terms*—Capacitance-to-frequency converter, r**elaxation **oscillator, capacitive sensor, microcontroller, Arduino Micro.**

I. INTRODUCTION

Capacitive sensors are used to convert nonelectrical physical or chemical quantities into capacitance. This makes it possible to measure, among others, moisture content [1]–[5], relative humidity [6]–[12], force [13], [14], pressure [15]–[17], liquid level [18]–[20], and even the mass of small quantities of water [21], steel surface corrosion [22], and atmospheric particulate matter [23] by measuring the capacitance of these sensors. To measure the value of the sensor's capacitance, its capacitance must be converted into a voltage (based on the capacitance-to-voltage techniques, as classified in [24]) or into a signal frequency (using one of the frequency modulation techniques that are a subset of the capacitance-to-time techniques, as described in [24]) using an electronic circuit. In the second case, relaxation oscillators are most often used, which generate a square (triangular) wave with a frequency that depends on the value of the sensor capacitance. Thus, in such a case, it is enough to measure the frequency of the signal and then convert its value into a value of capacitance or a given physical or chemical quantity. This task can be performed, e.g., by microcontrollers equipped with timers/counters [2]–[4], [14], [20], [24]–[29].

Based on the active components used to build the relaxation oscillators, they can be divided into those based on:

- operational amplifiers [1]–[3], [6], [12], [19], [25], [30]–[35], including those with comparators [26], [36], and including those with inverters [13], [14], [27],
- CCIIs [7], [37]–[39],
- CMOS inverter gates (NOT gates):
  - three-stage ring oscillators [8], [16], [17], [23], [40],
  - five-stage ring oscillators [9], [10], [41],
  - three-gate stable RC oscillators [20], [21],
- an IC 555 Timer [4], [5], [11], [18], [22].

A good solution for the interface circuit of the capacitive sensor, because it is very simple, is to use the well-known three-gate stable RC relaxation oscillator [42] as a capacitance-to-frequency converter circuit, because it can be built from only one 74xx digital logic integrated circuit, two reference resistors, and one capacitor (capacitive sensor), and, as shown in [21], it is characterized by a low noise level and low sensitivity to temperature changes [20].

As mentioned above, the microcontroller can measure the frequency of the signal generated by the relaxation oscillator, control the measurement system (in this case referred to as the smart sensor), and process and store the measurement results, and of course communicate with the environment via serial interfaces (e.g. UART, USB).

The paper proposes a new, complete approach to the development of smart capacitive sensors for sensors located close to the system integrating hardware, i.e., the interface circuit (the microcontroller and the relaxation oscillator) [42], with software, i.e., a measurement algorithm and a calibration algorithm with a calibration dictionary stored in the microcontroller's program memory. This solution includes the following novelties:

- Ability to measure the values of capacitive sensors from single picofarads and at least hundreds of picofarads, with a resolution of 0.0035% of the measured value and relative uncertainty of less than 0.012% based on the proposed simple hardware.
- Development of a frequency meter based on a microcontroller with at least two counters, including one 16-bit (hardware), with an adaptive measurement duration ensuring a measurement resolution of between $1/2^{15}$ and $1/2^{16}$ for the entire measurement range, which made it possible to measure capacitance with a resolution of 0.0035% of the measured value. It is based on a new measurement procedure (software).
- Development of a calibration method (a calibration algorithm and a calibration dictionary) and a method of determining the value of the capacitance based on the measured frequency. As a result, high measurement accuracy is achieved, as shown in the first point.
- Proposing criteria and a method of determining the value of the reference resistors of a relaxation oscillator depending on, inter alia, the range of the measured capacitance values and the measuring capabilities of the microcontroller.
- Using the popular HC240 series of octal buffers and line drivers instead of typical CMOS inverter gates (e.g. MC14049UB [21], 74HC06, etc.) to build the relaxation oscillator circuit. As a result, the microcontroller can be isolated from the sensor, which increases the reliability of its operation. This is an advantage of the proposed solution from a practical standpoint because the sensors are often outside the device casing and thus exposed to damage that could lead to damage to, e.g., the microcontroller which is the heart of the measurement system. We can also turn off the sensor circuit, which reduces the power consumption.

In addition, the paper presents a complete example of a smart sensor solution based on a popular Arduino Micro module [43], specifically the ATmega32U4 microcontroller [44], and one SN74HC540 octal buffer and line driver with a 3-state output [45].

The proposed approach was analyzed with the LTspice software and experimentally tested with the use of a set of silver mica capacitors with values from 1 pF to 300 pF, which includes, inter alia, the ranges of the capacitance values of humidity sensors [46]–[48].

II. Operating Principles

The logical structure of the smart sensor solution designed for microcontrollers for capacitive sensors is presented in Fig. 1. This solution is divided into two parts: the hardware part, which includes a microcontroller, a square wave generator with a capacitive sensor, and a communication system, and the software part, which is responsible for the system configuration, measurement control, communication control, and data processing.

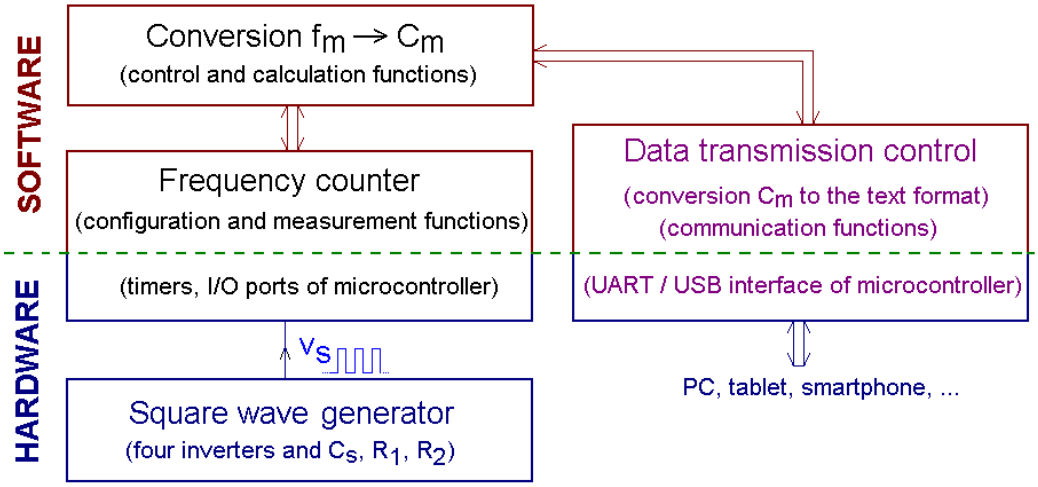

Fig. 1. Logical structure of the smart sensor solution designed for microcontrollers.

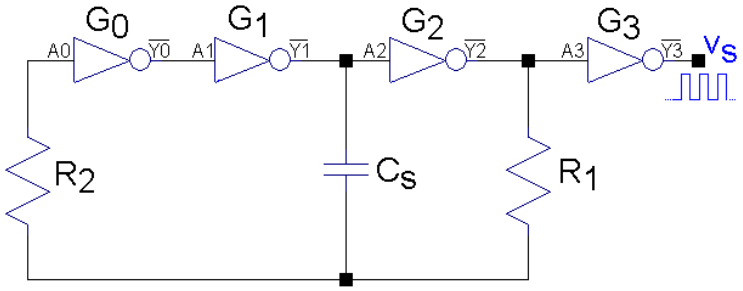

Fig. 2. Three-gate stable RC relaxation oscillator [42] based on an SN74HC540.

A. Square wave generator

The task of the relaxation oscillator shown in Fig. 2 is to generate a square wave v_s with a frequency f_s depending on the value C_s of the sensor's capacitance. In this case, the frequency f_s is approximately inversely proportional to the capacitance value C_s [42]:

$$f_s \cong \frac{1}{2 \cdot R_1 \cdot C_s \cdot \left(\frac{0.405 \cdot R_2}{R_1 + R_2} + 0.693 \cdot R_1 \right)} \tag{1}$$

where: R_1 and R_2 are reference resistors (Fig. 2).

If we assume that $R_1 = R_2 = R$, then:

$$f_s \cong \frac{0.559}{R \cdot C_s} \tag{2}$$

However, as demonstrated by simulation studies with the use of LTspice and preliminary experimental studies, formulas (1) and (2) are valid only for $C_s > 1$ nF, which means they are useless in the typical application of capacitive sensors. The relative error in determining the capacitance value is as high as about 1000% for 1 pF and decreases to about 25% for 300 pF. This is due to, inter alia, the delays introduced by the inverters not being taken into account (Fig. 2). For this reason, a new method for determining the value of the capacitance was developed, which is described in Section V.

B. Frequency meter based on a microcontroller

The microcontroller, together with the software, acts as a frequency meter and communication system and determines the value of the sensor capacitance based on the measured frequency. The concept of frequency measurement with the use of a microcontroller is shown in Fig. 3. Timer0 determines the duration of the measurement—the time t_{gate} in which the number of

pulses p_s generated by the relaxation oscillator is counted, i.e. as shown in Fig. 3, it controls the gate opening time t_{gate} by generating a v_{gate} pulse. An 8-bit counter/timer equipped with a prescaler is sufficient for this task.

However, a 16-bit counter/timer should be used for Timer1 to measure the f_s frequency to ensure the highest possible measurement resolution. Also, for this reason, the number of measured pulses p_s in the t_{gate} time should be as large as possible, i.e. in our case within the range from 2^{15} to 2^{16} for the entire frequency measurement range. Therefore, a new frequency measurement method with an adaptive measurement duration was developed. It will be illustrated on the example of an ATmega32U4 microcontroller that meets the above-mentioned requirements.

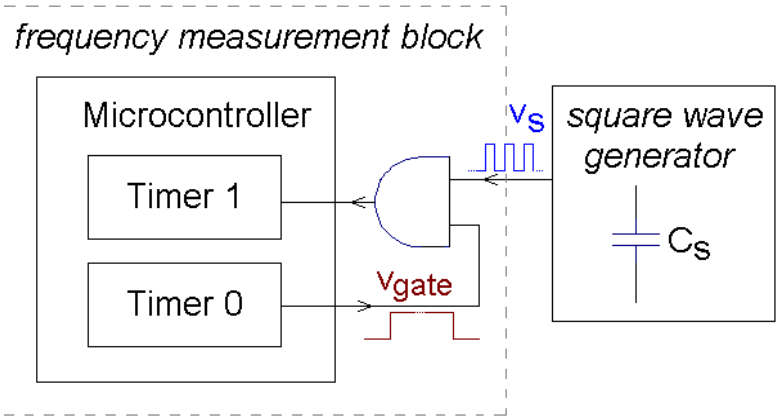

Fig. 3. Concept of frequency measurement based on a microcontroller equipped with two timers/counters.

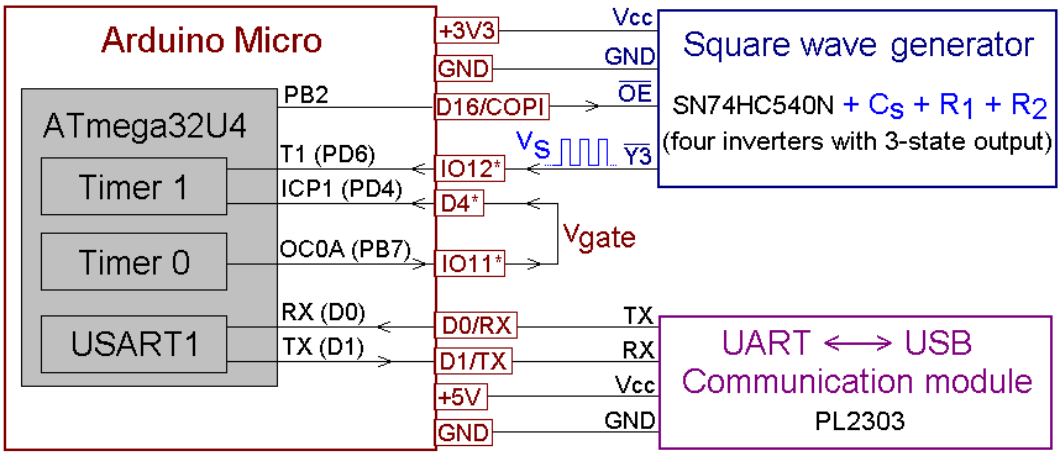

Fig. 4. Smart capacitive sensor based on an Arduino Micro module.

The complete smart sensor prototype based on this microcontroller is shown in Fig. 4. A PL2303 communication module [49] has been added to the system, which provides communication between the device and a PC.

As shown in Fig. 4, the AND gate from Fig. 3 is unnecessary due to the proposed measuring procedure, the algorithm of which is shown in Fig. 5. Timer0 generates a square wave v_{gate} with a period T_{gate}, the rising edges of which cause Timer1 to latch and save the current value of the counted pulses m_s of the v_s signal in the ICR1 register [44, page 117]. The period T_{gate} should be selected so that for the minimum value of the capacitance C_{s_min}, i.e. for the maximum value of the frequency f_{s_max}, at least two rising edges at the ICP1 input of Timer1 appear. The first value of m_s latched by the first edge denoted by m_{s_first} and the last value of m_s latched by the

m_{gate}-th edge of the v_{gate} signal are ultimately stored. Then the number of counted pulses p_s in the time $t_{gate} = m_{gate} \cdot T_{gate}$ is $p_s = m_{s\_first} - m_s$. Hence, the formula for the measured frequency f_s is as follows:

$$f_s = \frac{p_s}{m_{gate} \cdot T_{gate}} \tag{3}$$

The code of the frequency measurement procedure written in ANSI C is divided into the main function and two interrupt services (Fig. 5). In the main function, Timer0 and Timer1 are cleared and then started, while Timer0 works in CTC mode (Toggle OC0A on Compare Match) with the prescaler set to the value of clk/1024. Then T_{gate} = 5.12 ms, for the microcontroller clock frequency of f_{clk} = 16 MHz [43]. Timer1 works with the following settings: an external clock source on the T1 pin and counting on the rising edge, capture the value of

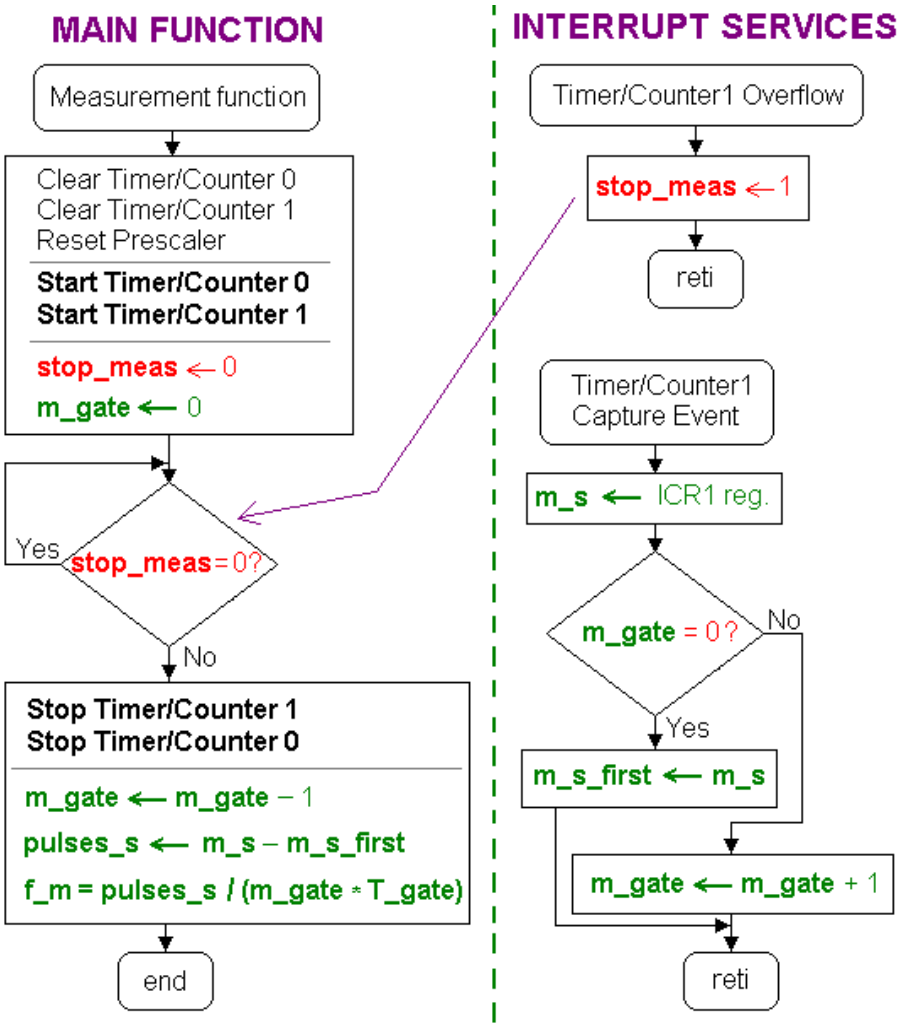

Fig. 5. Frequency measurement algorithm.

the counter at the rising edge at the ICP1 pin, and set Input Capture Noise Canceler [44, page 118]. Then, the *stop_meas* variable responsible for the control of the measurement duration is cleared, as well as the *m_gate* variable containing the current/final number of pulses counted on the ICP1 pin by the Timer/Counter1 Capture Event interrupt service. When the *stop_meas* variable is set in the Timer/Counter1 Overflow interrupt service, the main function stops Timer0 and Timer1 and calculates the frequency value based on the formula (3) using the values *m_s* and *m_s_first* saved by the Timer/Counter1 Capture Event interrupt service.

III. Determination of Reference Resistor Values of the Relaxation Oscillator

As already mentioned, the value of a frequency f_s of a signal v_s generated by the relaxation oscillator is primarily dependent on the C_s, R_1, R_2 values and the delay τ_d introduced by the inverters. The delay τ_d for a given integrated circuit and its operating conditions is constant and the range of changes in the capacitance values of the capacitive sensors C_s is also constant because it is set from C_{s_min} to C_{s_max}. Thus, the values of the desired frequency range can only be determined with the use of reference resistors R_1 and R_2.

The criterion that should be taken into account when selecting the values of these resistors is the limitation of the maximum value of the signal frequency f_s that can be fed to the input of the counter of the microcontroller. For each microcontroller, we can write the condition:

$$f_s < \xi \cdot f_{clk} \tag{4}$$

where: f_{clk}—system clock frequency of the microcontroller, ξ—constant resulting, inter alia, from the Nyquist sampling theorem.

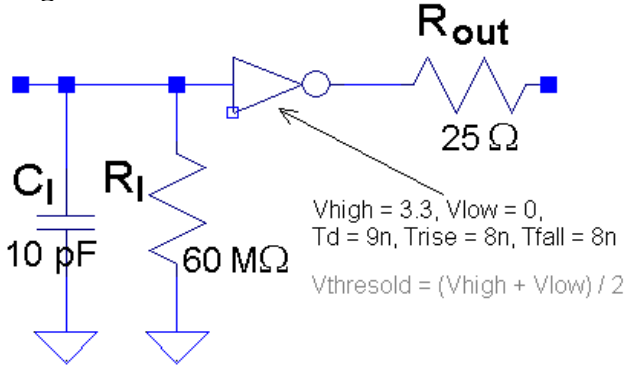

Fig. 6. Proposed model of the inverter of the SN74HC540 for LTspice.

For the Atmega32U4, it is 0.4 [44, page 93]. For example, for f_{clk} = 16 MHz [43], the values of f_s should be less than f_{s_max} = 6.4 MHz.

The inverter model shown in Fig. 6 was adopted for the LTspice simulation studies. The values of the input capacitance C_i, input resistance R_i, output resistance R_{out}, as well as rise T_{rise}, fall T_{fall}, and propagation T_d times were determined based on an analysis of the technical documentation of the SN74HC540 [45] and preliminary experimental tests.

The first conclusion was that the values of the resistors R_1 and R_2 should be equal so the amplitude of the triangular wave at the input A0 is as large as possible, which ensures a more reliable conversion of this waveform into a square wave by the inverter G0 (Fig. 2). Hence, an initial rough value of $R = R_1 = R_2$ can be determined based on formula (2), taking f_{s_max}, C_{s_min} for the calculations. Then, simulating the operation of the relaxation oscillator in LTspice, we select the values of R so condition (4) is met.

For practical reasons, it was assumed that the frequency could be measured even for the relaxation oscillator without a capacitance sensor ($C_{s,0}$ = 0 F). Hence, R = 10 kΩ was determined, then, for this value from the simulation, $f_{s,0}$ = 6.44 MHz, and from the measurements, $f_{m,0}$ = 6.11 MHz. Of course, we can choose a bigger R value, but this extends the measurement time, which increases the energy consumption of the system.

IV. Experimental results and discussion

A. Methods and materials

A prototype of the smart compact sensor shown in Fig. 4 was experimentally tested. R_1 = 10.021 kΩ, R_2 = 10.017 kΩ, and V_{cc} (+3V3) = 3.2927 V were measured by an Agilent 34410A, and a set $\{C_{s,i}\}_{i=1,\ldots,I}$ (I = 19) of silver mica capacitors emulating a capacitive sensor with values from $C_{s,1}$ = 1.0004 pF to $C_{s,19}$ = 293.12 pF was precisely measured by an Agilent 4263B and a Hewlett-Packard 16047A.

After each measurement made by the smart sensor, the measurement results were sent to a PC via a USB interface.

B. Testing the measuring accuracy of the frequency meter

In the first stage of the experimental research, only the frequency measurement system was tested. For this purpose, a square-wave signal generated by an Agilent 33250 was applied to the T1 input of the microcontroller. A signal was generated in the range from 62 kHz to 6.093 MHz, which corresponds to the range of frequencies generated by the relaxation oscillator for the assumed capacitance range of the sensor. 1024 independent measurements were performed for each frequency value. Based on these measurements, the maximum and minimum values of the relative errors δf of the frequency measurement were determined. The results are shown in Fig. 7.

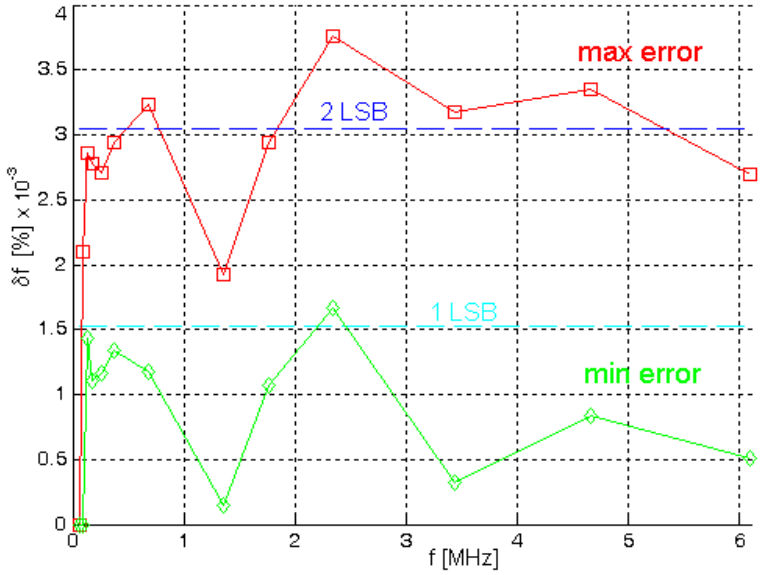

Fig. 7. Relative errors δf of the frequency measurement of the frequency meter in Fig. 4.

It can be seen from Fig. 7 that the relative error of frequency measurement δf is at the level of 0.0035% and is not much higher than the 2 LSB discretization error of the 16-bit counter, which is 0.00305%. Therefore, this value can be taken as the relative measurement accuracy of the measurement system.

C. Scaling of the measurement system

Also in this case, 1024 measurements of the frequencies of the signals generated by the relaxation oscillator were performed for each i-th capacitance value $C_{s,i}$. Then, from each i-th set of results, the maximum $f_{max,i}$, minimum $f_{min,i}$ and average $f_{m,i}$ values were determined. The values of the absolute error Δf_i (5) and the relative error δf_i (6) were also calculated:

$$\Delta f_i = f_{\max,i} - f_{\min,i} \tag{5}$$

$$\delta f_i = \frac{\Delta f_i}{f_{m,i}} \tag{6}$$

The results for the full range of capacitance values are shown in Fig. 8.

Fig. 8 shows that the relative error δf of the frequency measurement in the range from 12 pF to 300 pF is in the range of 2–3 LSB and does not exceed the value of 0.0084%, while for capacitances smaller than 12 pF, it is in the range 2–4 LSB, reaching a maximum relative error of 0.012%. Such a good result proves the high stability and accuracy of the frequency of the square wave generated by such a simple relaxation oscillator. Unfortunately, the disadvantage of this solution is the fact that it is impossible to write a simple formula for the relationship between the measured frequency f_s and the corresponding capacitance value C_s, as shown in Fig. 9, which shows graphs of the measurement data, data from the LTspice simulation, and data calculated from formula (1). However, this problem was solved by using a calibration method based on the calibration dictionary described in the next section.

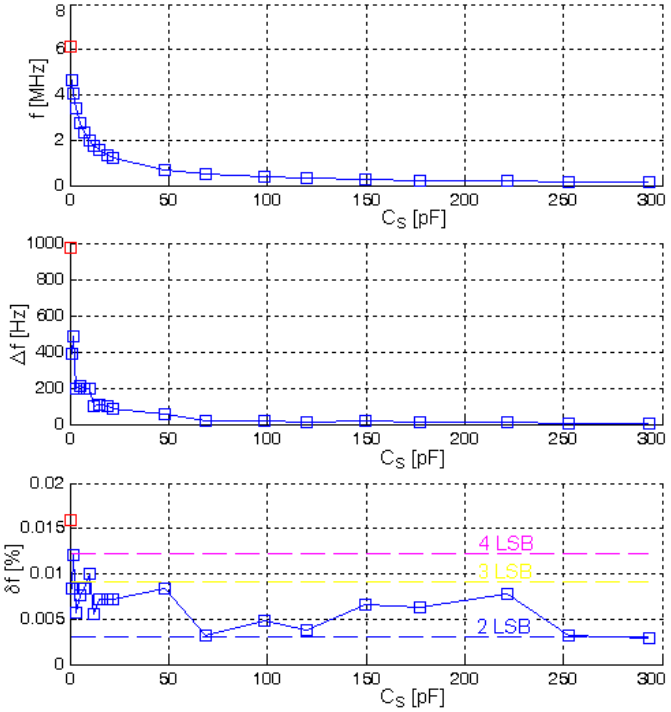

Fig. 8. Graphs of the measured average frequency f_m, absolute Δf, and relative δf errors as a function of the capacitance value C_s for the circuit in Fig. 2.

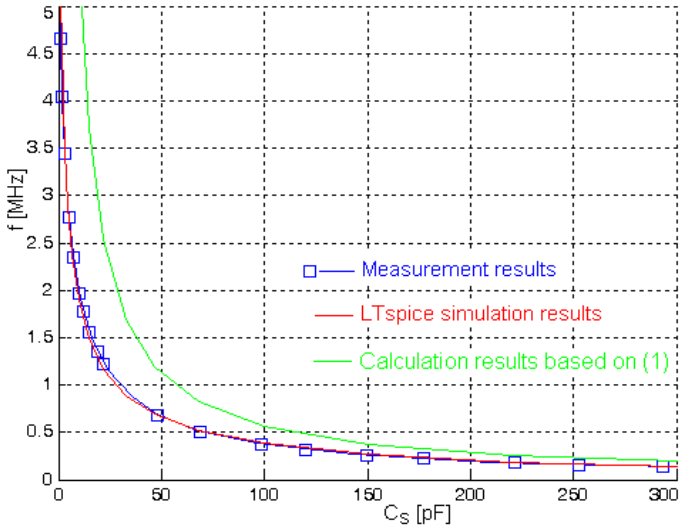

Fig. 9. Comparison of measurement results with simulation results from LTspice and based on formula (1).

The duration of a single measurement $t_{gate,i}$ was measured simultaneously with the frequency measurements. The results are presented in Fig. 10. The figure shows that this time for the assumed measurement resolution of Timer1, in our case 16-bit, is approximately linearly dependent on the capacitance value, and inversely proportional to the measured frequency f_s, which results from the measurement algorithm (Fig. 5). For example, for the assumed capacitance range C_{s_min} to C_{s_max} of the sensor and resistance values R_1 and R_2, the duration of a single measurement of the frequency f_s for an uncertainty level lower than 0.012% (Fig. 8) is in the range from 14 ms to 471 ms.

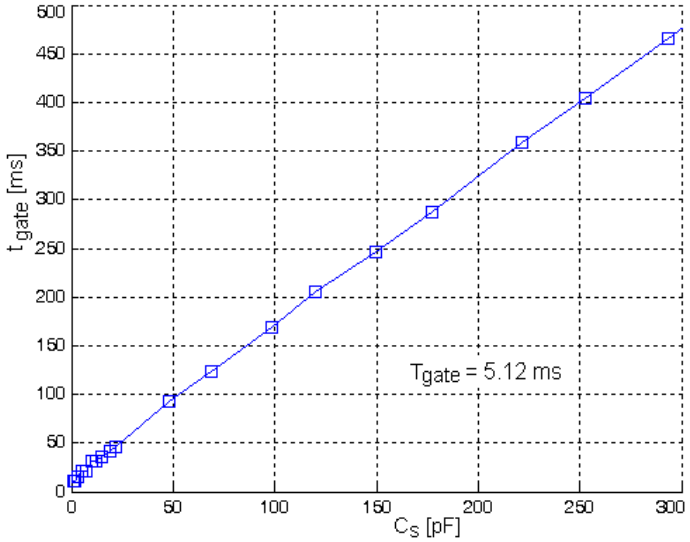

Fig. 10. Duration t_{gate} of a single measurement as a function of the capacitance value C_s for the assumed measurement accuracy ($2^{15} < m_s < 2^{16}$).

V. CALIBRATION METHOD

A calibration method is proposed to determine the capacitance value C_s based on the measured frequency f_s. It consists of two parts. The first part is performed once during system design or startup, during which a calibration dictionary is created, similar to [24], [50], and the second part uses this dictionary to determine the capacitance value of the sensor.

It should be remembered that the calibration should be performed under the target operating conditions of the circuit, i.e. for the same value of the supply voltage V_{cc}, and at the same or similar ambient temperature T_a.

The algorithm for creating the calibration dictionary is as follows:

1. For given reference values of $C_{s,i}$, in our case we used a set of silver mica capacitors, we measure M times the frequencies $f_{s,i}$, where $i = 1, \ldots, I$, and then determine the average value $f_{m,i}$. It is worth making $I = J \cdot K + 1$, where K is the number of splite functions that are polynomials of the J-th degree. The simulation research showed that the best approximation is obtained for square functions, hence $J = 2$. $K = 9$ was selected, thus $I = 19$.
2. Then a set of measurement points $\{(f_{m,i},C_{s,i})\}_{i = 1,\ldots, I}$ is divided into K subsets consisting of $J + 1$ points, where $K = (I - 1) / (J + 1)$. It was assumed that one knot is common to the neighboring functions, hence we have $I - 1$. So, for each $k = 1, \ldots, K$, we have three points with indexes $i = r + 2\cdot(k - 1)$, where $r = 1, 2, 3$.
3. So, e.g. using the polyfit Matlab function, for each k, we calculate a set of square function coefficients $\{a_{j,k}\}_{j = 1, 2, 3}$ based on three measurement points with indexes $1 + 2\cdot(k - 1)$, $2 + 2\cdot(k - 1)$, and $3 + 2\cdot(k - 1)$. We also determine the frequency thresholds $f_{max,k} = f_{3 + 2\cdot(k - 1)}$ that will be used to choose the k index in the algorithm for determining the measured capacitance value.

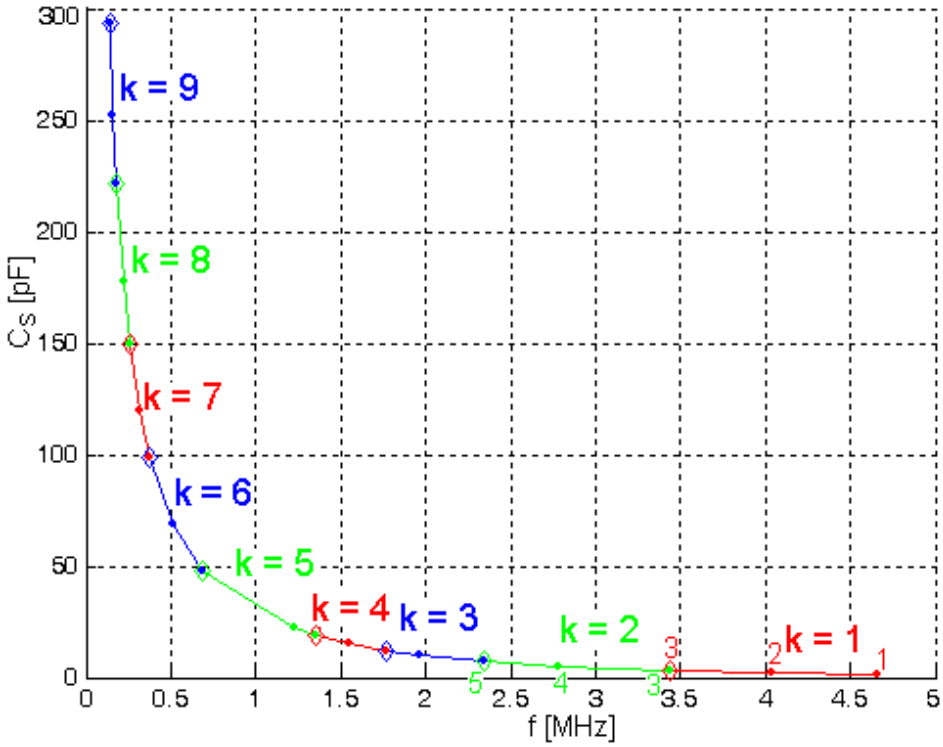

Fig. 11. Chart of the set of splite functions representing the calibration dictionary.

Thus, the calibration dictionary is in the form of $\{a_{j,k}, f_{max,k}\}_{j = 1, 2, 3;\ k = 1, \ldots, K}$, where $a_{j,k}$ is a double type variable (8 bytes), and $f_{max,k}$ is a long integer variable (4 bytes), hence the size of the dictionary for $K = 9$ is only 252 bytes. The chart of the set of splite functions representing the calibration dictionary is shown in Fig. 11.

In contrast, the algorithm for determining the value of C_s based on the measured f_s value and calibration dictionary consists of the following two steps:

1. We determine the k index so that the $f_s > f_{max,k}$ condition is met, where $f_{max,k}$ is the highest value from the set $\{f_{max,k}\}_{k = 1, \ldots, K}$ fulfilling this condition.
2. Then, using the value of f_s and index k, we calculate the value of C_s based on formula (7):

$$C_s = \sum_{j=1}^{J+1} a_{j,k} \cdot f_s^{j-1} \tag{7}$$

or its simpler form (8), which can be directly implemented, e.g., in ANSI C:

$$C_s = a_{1,k} + a_{2,k} \cdot f_s + a_{3,k} \cdot f_s \cdot f_s \tag{8}$$

It can be seen from (8) that calculating the value of C_s requires only three multiplication operations, two addition operations, and one assignment operation. Hence, the function written in ANSI C that performs these calculations occupies only 708 bytes in the program memory of the microcontroller. So, this function together with the calibration dictionary take up less than 1 KB of the 32 KB available [44, page 18].

As for the number M of the frequency measurements, it should be such that the standard deviation of the mean value of $f_{m,i}$ is less than the discretization error of the 16-bit counter. By assuming, for example, that the confidence interval is "4-sigma", it is enough if $M = 32$. However, we decided on such a large value of $M = 1024$ because the relative uncertainty of the standard deviation assessment is 2.2%, which allows for a precise statistical analysis of the results, and thus for an accurate assessment of the proposed method based on the experimental

data. Hence, the time of all measurements during the calibration process is about 1 min 24 s for M = 32 to 44 min 34 s for M = 1024.

TABLE I
COMPARISON OF THE SOLUTIONS BASED ON A THREE-GATE STABLE RC RELAXATION OSCILLATOR

References	**[20]**	**[21]**	**This work**
Range of capacitance values	1.069–2.076 nF	77–182 pF	1–300 pF
Relative uncertainty of measurement	0.6%	0.55%	0.012% (0.0084% for C_s > 12 pF)

VI. COMPARISON WITH THE STATE OF THE ART

In most applications of microcontrollers for measuring the capacitance of sensors, they are used to measure the pulse duration based on direct sensor-microcontroller interface methods [24], [26], [28], [29]. Similar approaches include measurement of the period of the square wave signal, e.g. based on measurements of the duration of the high and low states [25], and also based on a constant pulse counting method [27]. Other solutions include a method in which one counter counts the input pulses (in a period 60 s) while the other counter counts the interval clock pulse which is 1/12 of f_{clk} [20], and a method that used the counter in capture mode and is clocked by an internal 200 kHz signal [4]. In contrast, typical frequency measurement is used in [2], [3], where the pulses of a square wave are measured precisely for 1 s by the 8-bit TMR0 counter of a PIC16F877A microcontroller using its overflows.

Hence, the advantages of the proposed frequency meter based on a microcontroller over the above-mentioned methods are its simplicity of use and high measurement accuracy, full use of the capabilities of a 16-bit counter, and short (optimal) measurement time relative to the measured capacitance, e.g. ranging from 14 ms to 471 ms for the assumed measuring range of the capacitive sensor.

Table I summarizes the solutions for capacitive sensors based on the generation of a square wave with the use of a three-gate stable RC relaxation oscillator.

The table shows that the proposed approach, inter alia thanks to the use of the calibration method, enables the measurement of smaller capacitances starting from 1 pF, as opposed to the other methods. But, above all, it is characterized by a much lower relative measurement uncertainty, which is about 46 times smaller, or even 65 times smaller for the same capacitance ranges, than the relative measurement uncertainty for the methods presented in [20], [21].

At this point, it should also be mentioned that it has been proposed to build a relaxation oscillator based on the popular HC240 series of octal buffers and line drivers, which enables the sensor to be turned off, which can protect the system against damage and reduce energy consumption.

VII. MEASUREMENT UNCERTAINTY ANALYSIS

To analyze the measurement uncertainty of the sensor capacitance C_s, it was assumed then tested that the graph in Fig. 9 can be approximately described by the following rational function:

$$f_s \approx \frac{1}{c \cdot C_s + d} \tag{9}$$

where: c, d—coefficients determined, e.g., based on two points belonging to the graph in Fig. 9, e.g. for $C_{s,1}$ and $C_{s,10}$, c = 28618 s/F, d = 0.186 μs.

Based on analogy to formula (1) and the fact that the relaxation oscillator introduces a constant delay τ_d, it can be assumed (inferred) that the coefficients $c = 2 \cdot \gamma \cdot R$, and $d = \tau_d$. Hence:

$$f_s \approx \frac{1}{2 \cdot \gamma \cdot R \cdot C_s + \tau_d} \tag{10}$$

Where, in this case, the coefficients γ, R, and τ_d characterize the properties of the relaxation oscillator circuit.

So, the formula for C_s has the form:

$$C_s \approx \frac{1 - f_s \cdot \tau_d}{2 \cdot \gamma \cdot R \cdot f_s} \tag{11}$$

Therefore, the relative uncertainty δC_s of the indirectly measurable variable C_s can be given by a root-sum-square formula of relative uncertainties [51]–[53] of the circuit coefficients γ, R, τ_d, and the measured value f_s, whose formulas are as follows:

$$\delta C_s(\gamma) = \frac{\Delta\gamma}{\gamma} \tag{12}$$

$$\delta C_s(R) = \frac{\Delta R}{R} \tag{13}$$

$$\delta C_s(\tau_d) = \frac{-1}{1 - f_s \cdot \tau_d} \cdot f_s \cdot \Delta\tau_d \tag{14}$$

$$\delta C_s(f_s) = \frac{-1}{1 - f_s \cdot \tau_d} \cdot \frac{\Delta f_s}{f_s} \tag{15}$$

where the values of $\Delta\gamma$, $\Delta\tau_d$, and ΔR define the inaccuracy of the calibration of the capacitive sensor circuit, as γ, R, and τ_d characterize the electrical properties of the relaxation oscillator circuit built on a given integrated circuit and for given operating conditions, e.g. supply voltage V_{cc} or ambient temperature T_a. Thus, these values mainly depend on the stability of the operating conditions of the system.

For example, the LP2985-33DBVR voltage regulator mounted on the Arduino Micro module [43] with a load current $I_L < 1$ mA (this value is consumed by the relaxation oscillator circuit) has an output voltage tolerance of 1.5%, which gives a maximum voltage change in the range of ±0.05 V. This, in turn, changes the propagation time t_d of one inverter by a maximum of ±0.05 ns [45]. Hence, finally, for the assumed range of measured frequencies, the value of $\delta C_s(\tau_d)$ is smaller than 0.002–0.52% as shown in Fig. 12.

The voltage stability V_{cc} was measured to verify the actual effect of supply voltage variations on $\delta C_s(\tau_d)$. It was found that the voltage stability error is 0.1%, i.e. it is about 15 times lower than the catalog value, hence $\delta C_s(\tau_d)$ is also about 15 times smaller and can be neglected.

The uncertainty $\delta C_s(f_s)$ has a similar shape in the function of f_s as $\delta C_s(\tau_d)$. For the relative measurement accuracy of the measurement system $\Delta f_s / f_s = 0.0035\%$, its maximum values are in the range of 0.003–0.023%.

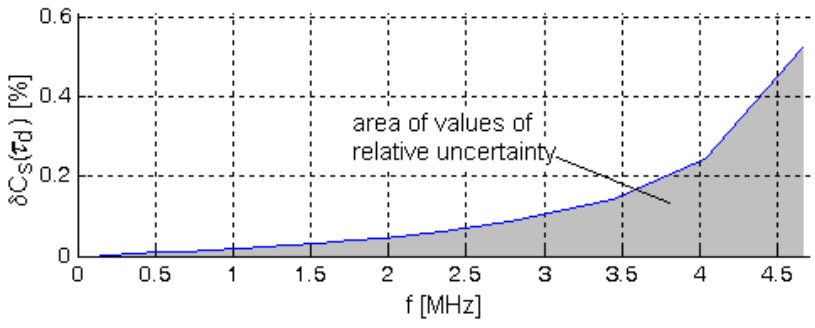

Fig. 12. Graph of the relative uncertainty $\delta C_s(\tau_d)$.

Formula (13) represents the tolerance of the resistors R_1 and R_2, and in fact their thermal drift in our case. As precision metal film resistors with a thermal drift of 0.0015% were used, a change in temperature, e.g., by about ±10°C, causes a change in the $\delta C_s(R)$ value at a level close to the maximum relative measurement error of f_s (Fig. 8).

Hence, the conclusion from the above considerations is that to maintain high measurement precision of the measurement of the sensor capacitance, the calibration of the system should take place in its target operating conditions, i.e. for a given supply voltage and the assumed ambient temperature range. For example, the prototype of the smart sensor was tested at T_a = 24 °C, which is currently intended for the precise measurement of capacitance at room temperatures. Of course, there is nothing to prevent the assignment of calibration dictionaries to individual ranges of operating temperatures. Then, e.g., after the microcontroller measures the temperature T_a, e.g. based on the method proposed in [54], the appropriate calibration dictionary generated for a given operating temperature range can be selected.

VIII. Conclusion

The report presented a new complete solution of a smart capacitive sensor for sensors located close to the system. The approach is designed for microcontrollers with at least one 8-bit counter/timer equipped with a prescaler, which determines the duration of the frequency measurement, and one 16-bit counter/timer used to count the number of pulses of the signal generated by a relaxation oscillator. A three-gate stable RC circuit built on an SN74HC540 octal buffer and line driver was used as the relaxation oscillator, which works as a capacitance-to-frequency converter.

The proposed solution also includes software that performs frequency measurement with an adaptive measurement time and determines the value of the sensor capacitance based on a calibration method that uses a calibration dictionary and communicates with a PC. It was written in ANSI C for a very common 8-bit microcontroller mounted on an Arduino Micro/Leonardo module.

It should also be noted that the method is based on simple hardware and software, as described above, which makes it easy to implement, which is a big advantage from a practical point of view.

The experimental studies confirmed that the relative capacitance measurement errors introduced by the proposed measurement system, among others thanks to the calibration method, are less than 0.012% for values smaller than 12 pF, and less than 0.0084% for values from 12 pF to 300 pF, which, for example, for 1 pF gives a resolution of about 0.12 fF.

References

[1] T. Islam, S. A. Khan, M. F. A. Khan and S. C. Mukhopadhyay, "A Relaxation Oscillator-Based Transformer Ratio Arm Bridge Circuit for Capacitive Humidity Sensor," *IEEE Transactions on Instrumentation and Measurement*, vol. 64, no. 12, pp. 3414–3422, Dec. 2015.

[2] T. Islam, A. U. Khan, J. Akhtar and M. Z. U. Rahman, "A Digital Hygrometer for Trace Moisture Measurement," *IEEE Transactions on Industrial Electronics*, vol. 61, no. 10, pp. 5599–5605, Oct. 2014.

[3] A. Ulla Khan, T. Islam and J. Akhtar, "An Oscillator-Based Active Bridge Circuit for Interfacing Capacitive Sensors With Microcontroller Compatibility," *IEEE Transactions on Instrumentation and Measurement*, vol. 65, no. 11, pp. 2560–2568, Nov. 2016.

[4] S. K. Korkua, S. Sakphrom, "Low-cost capacitive sensor for detecting palm-wood moisture content in real-time," *Heliyon*, vol. 6, issue 8, Aug. 2020, Art. no. e04555.

[5] P. Placidi, L. Gasperini, A. Grassi, M. Cecconi, A. Scorzoni, "Characterization of Low-Cost Capacitive Soil Moisture Sensors for IoT Networks," *Sensors*, June 2020, Art. no. 12: 3585.
[6] A. De Marcellis, C. Reig, M.-D Cubells-Beltrán, "A Capacitance-to-Time Converter-Based Electronic Interface for Differential Capacitive Sensors," *Electronics*, vol. 8, Jan. 2019, Art. no. 1: 80.
[7] S. Malik, K. Kishore, Artee, S. A. Akbar, T. Islam, "A CCII-based relaxation oscillator as a versatile interface for resistive and capacitive sensors," in *Proc. 3rd International Conference on Signal Processing and Integrated Networks*, 2016, pp. 359–363.
[8] C-L. Dai, "A capacitive humidity sensor integrated with micro heater and ring oscillator circuit fabricated by CMOS-MEMS technique," *Sensors and Actuators B: Chemical*, vol. 122, issue 2, pp. 375–380, March 2007.
[9] M-Z. Yang, C-L. Dai, D-H. Lu, "Polypyrrole Porous Micro Humidity Sensor Integrated with a Ring Oscillator Circuit on Chip," *Sensors*, vol. 10, Nov. 2010, Art. no. 11:10095–10104.
[10] M.-Z. Yang, C.-L. Dai, C.-C. Wu, "Sol-Gel Zinc Oxide Humidity Sensors Integrated with a Ring Oscillator Circuit On-a-Chip," *Sensors*, Oct. 2014, Art. no: 11:20360–20371.
[11] Saima Shaikh, M. Shahid Shaikh, Pinial Khan Butt, Farah Naveen Issani, Kehkahan Asma, "Embedded low Cost Solution of Remotely Sensing Humidity," *Indian Journal of Science and Technology*, vol. 11, issue: 14, pp. 1–5, April 2018.
[12] A. De Marcellis, G. Ferri, P. Mantenuto, "Uncalibrated operational amplifier-based sensor interface for capacitive/resistive sensor applications," *IET Circuits, Devices and Systems*, vol. 9, issue 4, pp. 249–255, July 2014.
[13] R. A. Brookhuis, T. S. J. Lammerink, R. J. Wiegerink, "Differential capacitive sensing circuit for a multi-electrode capacitive force sensor," *Sensors and Actuators A: Physical*, vol. 234, pp. 168–179, Oct. 2015.
[14] R. A. Brookhuis, R. J. Wiegerink, T. S. J. Lammerink, G. J. M. Krijnen, "Three-axial force sensor with capacitive read-out using a differential relaxation oscillator," in *Proc. Sensors, 2013 IEEE*, Nov. 2013, pp. 1–4.
[15] W. Jung, S. Jeong, S. Oh, D. Sylvester, D. Blaauw, "27.6 A 0.7pF-to-10nF fully digital capacitance-to-digital converter using iterative delay-chain discharge," in *Proc. 2015 IEEE International Solid-State Circuits Conference - (ISSCC) Digest of Technical Papers*, Feb. 2015, pp. 1–3.
[16] F. Deng, Y. He, X. Wu, Z. Fu, "A CMOS pressure sensor with integrated interface for passive RFID applications," *Measurement Science and Technology*, vol. 25, Oct. 2014, Art. no. 125104.
[17] C-L. Dai, P-W. Lu, C. Chang, C-Y. Liu, "Capacitive micro pressure sensor integrated with a ring oscillator circuit on chip," *Sensors (Basel)*, vol. 9, issue 12, pp. 10158–10170, Dec. 2009.
[18] K. V. Santhosh, Blessy Joy, Swetha Rao, "Design of an Instrument for Liquid Level Measurement and Concentration Analysis Using Multisensor Data Fusion," *Journal of Sensors*, vol. 2020, Jan. 2020, Art. no. 4259509.
[19] F. Reverter, X. Li, G. C.M. Meijer, "Liquid-level measurement system based on a remote grounded capacitive sensor," *Sensors and Actuators A: Physical*, vol. 138, issue 1, pp. 1–8, April 2007.
[20] K. Praveen, M. P. Rajiniganth, A. D. Arun, P. Sahoo, S. A. V. Satya Murty, "A novel technique towards deployment of hydrostatic pressure based level sensor in nuclear fuel reprocessing facility," *Review of Scientific Instruments*, vol. 87, Feb. 2016, Art. no. 025111.

[21] R. N. Dean, A. K. Rane, "A Digital Frequency-Locked Loop System for Capacitance Measurement," *IEEE Transactions on Instrumentation and Measurement*, vol. 62, no. 4, pp. 777–784, April 2013.
[22] H.K. Twigg, M. Molinari, "Test results for a capacitance-based corrosion sensor," in *Proc. of the Thirteenth International Conference on Condition Monitoring and Machine Failure Prevention Technologies*, Paris, France, Oct. 2016.
[23] U. Ferlito, A. D. Grasso, M. Vaiana, G. Bruno, "Integrated Airborne Particle Matter Detector," in *Proc. 2019 26th IEEE International Conference on Electronics, Circuits and Systems (ICECS)*, Nov. 2019, pp. 95–96.
[24] Z. Czaja, "Measurement method for capacitive sensors for microcontrollers based on a phase shifter," *Measurement*, vol. 192, March 2022, Art. no. 110890.
[25] T. Gasosoth, T. Lianghiranthaworn, S. Unai, "A period-based measurement for grounding capacitance meter with arduino using a relaxation oscillator," *Journal of Physics: Conference Series*, vol. 1380, June 2019, Art. no. 012074.
[26] F. Reverter, X. Li, G. C M Meijer, "A novel interface circuit for grounded capacitive sensors with feedforward-based active shielding," *Measurement Science and Technology*, vol. 19, Jan. 2008, Art. no. 025202.
[27] M. Gasulla, Xiujun Li, G. C. M. Meijer, "The noise performance of a high-speed capacitive-sensor interface based on a relaxation oscillator and a fast counter," *IEEE Transactions on Instrumentation and Measurement*, vol. 54, no. 5, pp. 1934–1940, Oct. 2005.
[28] Z. Czaja, "A measurement method for capacitive sensors based on a versatile direct sensor-to-microcontroller interface circuit," *Measurement*, vol. 155, April 2020, Art. no. 107547.
[29] Z. Czaja, "A measurement method for lossy capacitive relative humidity sensors based on a direct sensor-to-microcontroller interface circuit," *Measurement*, vol. 170, Jan. 2021, Art. no. 108702.
[30] T. Tyagi, P. Sumathi, "Capacitive and resistive sensing based on compensated relaxation oscillator," in *Proc. 6th International Conference on Computer Applications In Electrical Engineering-Recent Advances (CERA)*, Oct. 2017, pp. 98–102.
[31] T. Islam, "Advanced interfacing techniques for the capacitive sensors". In *Advanced Interfacing Techniques for Sensors*, Springer, 2017, SSMI 25, pp. 73–109.
[32] T. Tyagi, P. Sumathi, "Frequency estimation techniques in capacitance-to-frequency conversion measurement," *Review of Scientific Instruments*, vol. 91, Jan. 2020, Art. no. 015005.
[33] L. Areekath, B. George, F. Reverter, "A Closed-Loop Capacitance-to-Frequency Converter for Single-Element and Differential Capacitive Sensors," *IEEE Transactions on Instrumentation and Measurement*, vol. 69, no. 11, pp. 8773–8782, Nov. 2020.
[34] U. Ferlito, A. D. Grasso, S. Pennisi, M. Vaiana, G. Bruno, "Sub-Femto-Farad Resolution Electronic Interfaces for Integrated Capacitive Sensors: A Review," *IEEE Access*, vol. 8, pp. 153969–153980, Aug. 2020.
[35] Qi Jia, G. C. M. Meijer, Xiujun Li, Chao Guan, "An integrated interface for grounded capacitive sensors," *Sensors, 2005 IEEE*, Nov. 2005, Art. no. 1597890.
[36] V. Sreenath, B. George, "An Improved Closed-Loop Switched Capacitor Capacitance-to-Frequency Converter and Its Evaluation," *IEEE Transactions on Instrumentation and Measurement*, vol. 67, no. 5, pp. 1028–1035, May 2018.
[37] Muhammad Taher Abuelma'atti, Munir Ahmad Al-Absi, "A current conveyor-based relaxation oscillator as a versatile electronic interface for capacitive and resistive sensors," *International Journal of Electronics*, vol. 92, issue 8, pp. 473–477, Aug. 2005.

[38] S. Malik, K. Kishore, D. Sharma, M. Maharana, S. A. Akbar, T. Islam, "A CCII-based wide frequency range square/triangular wave generator," in *Proc. 2015 IEEE 2nd International Conference on Recent Trends in Information Systems (ReTIS)*, July 2015, pp. 446–449.
[39] L. Polak, R. Sotner, J. Petrzela, J. Jerabek, "CMOS Current Feedback Operational Amplifier-Based Relaxation Generator for Capacity to Voltage Sensor Interface," *Sensors*, vol. 18, issue 12, Dec. 2018, Art. no. 4488.
[40] K. Mohammad, D. J. Thomson, "Differential Ring Oscillator Based Capacitance Sensor for Microfluidic Applications," *IEEE Transactions on Biomedical Circuits and Systems*, vol. 11, no. 2, pp. 392–399, April 2017.
[41] A. Quintero, F. Cardes, L. Hernandez, C. Buffa, A. Wiesbauer, "A Capacitance-to-Digital Converter Based on a Ring Oscillator with Flicker Noise Reduction," in *Proc. 2016 Austrochip Workshop on Microelectronics (Austrochip)*, Oct. 2016, pp. 40–44.
[42] Fairchild Semiconductor. (October 1974). *Application Note 118, CMOS Oscillators.* [Online]. Available: https://www.changpuak.ch/electronics/ datasheets/AN-118.pdf
[43] Arduino Micro [Online]. Available: https://store.arduino.cc/ products/arduino-micro
[44] Atmel Corporation. (2016). *ATmega16U4/ATmega32U4 8-bit Microcontroller with 16/32K bytes of ISP Flash and USB Controller*. [Online] Available: https://ww1.microchip.com/downloads/en/ DeviceDoc/Atmel-7766-8-bit-AVR-ATmega16U4-32U4_Datasheet.pdf
[45] Texas Instruments. (2022). *SNx4HC540 Octal Buffers and Line Drivers With 3-State Outputs*. [Online]. Available: https://www.ti.com/ product/SN54HC540?qgpn=sn54hc540
[46] TE Connectivity Ltd. (2015). *HS1101LF Relative Humidity Sensor*. [Online]. Available: https://www.te.com/commerce/DocumentDelivery/ DDEController?Action=showdoc&DocId=Data+Sheet%7FHPC052_J%7FA%7Fpdf%7FEnglish%7FENG_DS_HPC052_J_A.pdf
[47] Vishay BCComponents. (2009). *2381 691 90001/HUMIDITY-SENS-E*. [Online]. Available: https://www.vishay.com/docs/29001/23226919.pdf
[48] Innovative Sensor Technology. *P14 Rapid Capacitive Humidity Sensor*. [Online]. Available: https://www.ist-ag.com/sites/default/files/dhp14-rapid_e.pdf
[49] Waveshare Electronics. (2013). *USB TO UART solution with USB Type A connector*. [Online]. Available: http://www.waveshare.com/w/ upload/a/ac/PL2303-USB-UART-Board-Schematic.pdf
[50] W. Toczek, Z. Czaja, "Diagnosis of fully differential circuits based on a fault dictionary implemented in the microcontroller systems," *Microelectronics Reliability*, vol. 51, issue 8, pp. 1413–1421, Aug. 2011.
[51] K. Kolikov, G. Krastev, Y. Epitropov, D. Hristozov, "Analytically determining of the absolute inaccuracy (error) of indirectly measurable variable and dimensionless scale characterising the quality of the experiment," *Chemometrics and Intelligent Laboratory Systems*, vol. 102, issue 1, pp. 15–19, May 2010.
[52] I. Farrance, R. Frenkel, "Uncertainty of measurement: A review of the rules for calculating uncertainty components through functional relationships," *The Clinical Biochemist Reviews*, vol. 33, pp. 49–75, May 2012.
[53] A. Buscarino, L. Fortuna, M. Frasca, Essentials of Nonlinear Circuit Dynamics with MATLAB® and Laboratory Experiments, 1st Edition, RC Press, Inc., 2017.
[54] Z. Czaja, "An Implementation of a Compact Smart Resistive Sensor Based on a Microcontroller with an Internal ADC," *Metrology and Measurement Systems*, vol. 23, issue 2, pp. 255–238, June 2016.